

# Optimizing the Radiation Treatment Planning of Brain Tumors by Integration of Functional MRI and White Matter Tractography

Arman Boroun (MSc)<sup>1</sup>, Hamid Gholamhosseinian (PhD)<sup>2</sup>, Alireza Montazerabadi (PhD)<sup>2</sup>, Seyed Hadi Molana (MD)<sup>3</sup>, Fakhreh Pashaei (PhD)<sup>1\*</sup>

<sup>1</sup>Radiation Sciences Research Center (RSRC), Aja University of Medical Sciences, Tehran, Iran

<sup>2</sup>Medical Physics Research Center, Mashhad University of Medical Sciences, Mashhad, Iran

<sup>3</sup>Department of Radiation Oncology, Aja University of Medical Sciences, Tehran, Iran

## ABSTRACT

**Background:** Diffusion tensor imaging (DTI) and functional magnetic resonance imaging (fMRI) present the ability to selectively protect functional regions and fiber tracts of the brain when brain tumors are treated with radiotherapy.

**Objective:** This study aimed to assess whether the incorporation of fMRI and DTI data into the radiation treatment planning process of brain tumors could prevent the neurological parts of the brain from high doses of radiation.

**Material and Methods:** In this investigational theoretical study, the fMRI and DTI data were obtained from eight glioma patients. This patient-specific fMRI and DTI data were attained based on tumor location, the patient's general conditions, and the importance of the functional and fiber tract areas. The functional regions, fiber tracts, anatomical organs at risk, and the tumor were contoured for radiation treatment planning. Finally, the radiation treatment planning with and without fMRI & DTI information was obtained and compared.

**Results:** The mean dose to the functional areas and the maximum doses were reduced by 25.36% and 18.57% on fMRI & DTI plans compared with the anatomical plans. In addition, 15.59% and 20.84% reductions were achieved in the mean and maximum doses of the fiber tracts, respectively.

**Conclusion:** This study demonstrated the feasibility of using fMRI and DTI data in radiation treatment planning to maximize radiation protection of the functional cortex and fiber tracts. The mean and maximum doses significantly decreased to neurologically relevant brain regions, resulting in reducing the neuro-cognitive complications and improving the patient's quality of life.

**Citation:** Boroun A, Gholamhosseinian H, Montazerabadi A, Molana SH, Pashaei F. Optimizing the Radiation Treatment Planning of Brain Tumors by Integration of Functional MRI and White Matter Tractography. *J Biomed Phys Eng.* 2023;13(3):239-250. doi: 10.31661/jbpe.v0i0.2210-1547.

## Keywords

Brain Neoplasms; fMRI; Diffusion Tensor Imaging; Radiation Therapy; Glioma; MRI

## Introduction

**G**liomas are considered the largest group of primary intracranial tumors and one-third of all primary tumors [1]. However, Low-grade Gliomas (LGGs) are typically slow-growing primary brain tumors, they have a very heterogeneous clinical behavior [2]. Compared with LGGs, High-grade Gliomas (HGGs) have a poor prog-

\*Corresponding author:  
Fakhreh Pashaei  
Radiation Sciences Research Center (RSRC),  
Aja University of Medical Sciences, Tehran, Iran  
E-mail: fakhreh.pashae@gmail.com

Received: 3 October 2022  
Accepted: 20 December 2022

nosis, a higher degree of malignancy, and difficulty in controlling [3]. In addition, gliomas represent 80% of all malignant primary brain tumors, treated with some therapeutic strategies, including surgery, radiotherapy, chemotherapy, or combinations [3].

Three-dimensional Conformal Radiation Therapy (3DCRT) is recognized as the standard therapy for glioma patients, including high-dose megavoltage-range radiation to the tumor [4,5]. Approximately, half of the patients survive more than 6 months, and many patients achieve long-term control or cure [5]. Cranial radiation can cause acute and chronic damage to various cells, resulting in demyelination and necrosis of the brain regions [6]. Neurocognitive dysfunction is one of the main side effects of cranial irradiation that seriously affects cognitive function and Quality of Life (QOL) [7,8]. In 50-90% of patients, receiving fractional radiotherapy, cognitive dysfunctions related to memory, executive functions, sustained attention, and information processing speed has been observed [5,9].

However, recent advances in multimodality treatment protocols have significantly improved the survival rates of patients with brain tumors [10,11], conformal radiotherapy (CRT) directly damages white and grey matter by causing inflammation, angiogenesis, and cell death [12]. The identification, characterization, and minimization of specific side effects, especially those related to functional sequelae, can seriously affect the QOL [13].

The prevention or minimization of radiotherapy-induced cognitive dysfunction is considered a topic of intense research for a long time [14]. Some successful strategies to reduce neurocognitive dysfunction side effects include radiotherapy prevention in children and a decrease in radiation dose to brain volume [15].

Modern radiation treatment plans are based on a conventional Magnetic Resonance Imaging (MRI) scan co-registration with a planning Computerized Tomography (CT). Integrating

functional imaging and white matter tractography for fractionated radiotherapy planning is slowly progressing in brain tumors [14]. When radiotherapy techniques combine with advanced imaging, such as functional MRI (fMRI) and Diffusion Tensor Imaging (DTI), they can bypass potential brain areas involved in neurocognitive functions [14]. The functional areas of the brain and white matter fiber pathways can be well-imaged using modern MRI technology [16]. Blood Oxygen Level-dependent (BOLD) fMRI and white matter tractography are used to identify functional structures and white-matter pathways of the brain, respectively, as critical volumes in treatment planning [17,18]. Integrating these modern techniques into radiation treatment plans could help spare healthy and sensitive brain areas from high-dose radiation [17-19]. When the tumor is located in critical regions, nearby functional structures and white matter pathways can receive radiation doses beyond their tolerance limits since they cannot be easily identified on anatomical CT/ MRI images. Functional neuroimaging, including BOLD and white matter tractography, can identify functional structures and white matter pathways; these imaging techniques are implemented in the radiation treatment plans to prevent the beam from passing through nearby critical areas, resulting in reduced radiation doses [20].

This investigation aimed to selectively protect the functional and neural pathways in patients with primary brain tumors by integrating fMRI and white matter tractography into the 3DCRT.

## Material and Methods

### Patients

This investigational theoretical study defines the possibility of integrating the fMRI and DTI data into radiation treatment planning. According to pre-operative MRI scans, 8 suspected glioma patients (two and six male and

female patients, respectively, aged from 21 to 63), who are scheduled for tumor resection and provided their informed consent, were recruited from December 2019 to June 2020. Moreover, in the current study, the glioma tissues included four LGGs (WHO Grade II) and four high-grade gliomas (WHO Grade IV).

All patients underwent pre-radiotherapy fMRI, DTI, and conventional MRI. Functional structures and white-matter pathways were placed in the natural regions without any overlap with the target volume of the lesions. All patients could perform specific tasks to generate functional maps of brain activation. The Varian linear accelerator with a Millennium dynamic multileaf collimator (DMLC) system delivered external radiation therapy.

### Patient preparation and MRI test considerations

The MR scanning sequence started by screening the patient for any clothing, jewelry, or devices, such as pacemakers that may degrade the MRI, its safety, and the patient's condition evaluation. The technologist explained the scanning procedure and answered questions. Patients were advised not to move at all during the examination with as much as possible fixed-position heads. The difficulty and simplicity of implementation were prioritized for the paradigms. Firstly, a paradigm with more patient attention is needed to achieve the desired outcomes; simpler paradigms are then adopted, such as finger movement implementation.

### Data acquisition

Three imaging studies were performed on the patients using a Siemens MAGNETOM Avanto (Siemens, Erlangen, Germany) 1.5 T scanner with an eight-channel head coil.

#### Anatomical and fMRI characteristics

T1-weighted structural brain MR Images were initially obtained using the MP-RAGE sequence (Repetition Time (TR)=1820 ms, Echo Time (TE)=3.49 ms, Inversion Time

(TI)=1100 ms, slice thickness=1 mm, number of slice=176, flip angle=7°, acquisition matrix=256×256 pixels). BOLD fMRI data were acquired to provide brain activation maps, using single-shot gradient echo-planar imaging (EPI) (TR=3000 ms, TE=30 ms, slice thickness=3 mm, number of slice=176, flip angle=90°, acquisition matrix=65×64 pixels), which is more sensitive to  $T_2^*$  changes.

#### Diffusion Tensor Imaging (DTI)

DTI images were acquired with the spin echo-echo planar imaging (SE-EPI) sequence (TR=9500 ms, TE=90 ms, acquisition matrix=128×128 pixels; FOV=256 mm×256 mm; slice thickness=2.0 mm; b value of 1,000 s/mm<sup>2</sup> along 12 non-collinear directions).

#### Experimental Paradigms

This study simulated the primary motor cortex, Broca's area, and Wernicke's area. The motor cortex, located in the precentral gyrus, is mainly responsible for the actual performance of movements [21]. Broca's area, placed in the frontal lobe (often left), produces speech. In contrast, Wernicke's area in the temporal lobe (usually the left side) is related to language comprehension and speech planning [22].

The hand, foot, lip, and tongue motor paradigms activated the primary motor cortex. The measurement sequence of these paradigms consisted of a 24-second activation period (8 scans) followed by a 24-second rest period (8 scans), with eight-time repeats. All the measurements started with an initial rest period.

The Reverse Word Reading (RWR) paradigm was used to stimulate Broca's area. The stimuli of the RWR task in each activation block consisted of 10-word trials in 24 s, followed by a 24-second rest period. The Persian five-letter word was presented for every individual in each activation period while the letters were displayed in reverse order. The individual was then asked to read each word silently once; the measurements always began with an initial rest period [23]. The story paradigm was used to stimulate Wernicke's area and started with a rest period. In the story paradigm, a short and

manageable story was first considered, which was broadcast through the device's audio system during a 33-second activation period (11 scans) followed by a 33-second rest period (11 scans), and these periods were repeated five times. The story was selected so that the story would end with the end of the paradigm.

## Data Analysis

### fMRI Data Analysis

After imaging, data were transferred to the MATLAB workstation for analysis using SPM12 software (Statistical Parametrical Mapping, Wellcome Department of Cognitive Neurology, London, England). Data series were motion-corrected and smoothed with a 6 mm Full Width at Half Maximum (FWHM) Gaussian kernel. The model function was applied to each voxel in the brain (general linear model), and a statistical map was finally estimated. Activated voxels were significantly identified using an initial  $P$ -value threshold of 0.001. The fMRI scan data (mean image) was combined with the T1 structural MRI image obtained at the same scanning position, leading to the visibility of the functional MR activation color map on the patient's brain anatomy. The merged image sets (JPEG format) were then converted into Digital Imaging and Communications in Medicine (DICOM)

format using MATLAB version 8.3 (R2014a). In this conversion, the color images were replaced with the grayscale images using the intensity of the green color as the grayscale intensity. The fMRI DICOM series were also sent to the planning system.

### DTI Analysis

Data pre-processing consisting of raw data conversion, skull-stripping, and motion/eddy correction was performed using DSI studio software (developed by Fang-Cheng Yeh from the Advanced Biomedical MRI Lab, National Taiwan University Hospital, Taiwan, Supported by Fiber Tractography Lab, University of Pittsburgh, and made available at <http://dsistudio.labsolver.org/Download/>). After data pre-processing, a reconstruction model base (DTI) was used to process the diffusion images. Average DTI values were extracted from voxels within the Regions of Interest (ROIs) and tracts. The tractography process used a deterministic fiber tracking algorithm. Desired neural pathways were extracted in two directions in two hemispheres of the brain. Finally, the location of fiber tracts, saved as the ROI, was determined on the T1 structural images by using 3D Slicer software.

### Image Fusion

As shown in Figure 1, each patient's axial

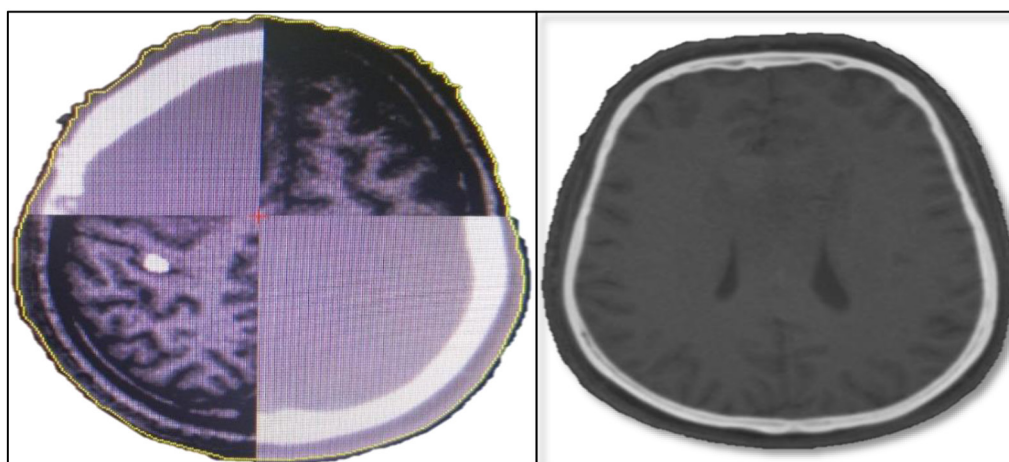


**Figure 1:** T1-weighted magnetic resonance imaging (MRI) and the corresponding axial computed tomography (CT) after registration

CT image was registered with the corresponding anatomical MRI images, using the automatic registration algorithm of the treatment planning system (TPS) to precisely describe the targets and standard organs at risk (OARs). The anatomical MRI volumes were fused with the corresponding white matter tracts and fMRI activation maps and then imported into the Isogray TPS software version 3.1 as separate grayscale DICOM images.

### Treatment Planning

The prescribed dose was 54 Gy to 60 Gy. Anatomical OARs, including the brainstem, spinal cord, eyes, bilateral lens, bilateral retina, lacrimal glands, bilateral cochlea, bilateral optic nerves, and the optic chiasm were delineated. The fiber tracts and the functional structures nearby the targets were also contoured as extra OARs using the fused fMRI and DTI images. Two 3DCRT treatment plans were developed for each patient. In the first plan, only the planning target volume (PTV) and anatomical OARs were considered. On the other plan, the physicist took the functional structures and fiber tracts situated near the target as neuro-cognitive functions OARs. The second plan was generated to reduce the dose of the functional structures and fiber tracts while keeping prescription dose coverage for the PTV and similar OAR dose-volume levels as the stan-

dard care treatment plan.

Dose-volume histograms (DVH) data were extracted from TPS. The mean and maximum doses ( $D_{\text{mean}}$  &  $D_{\text{max}}$ ) of radiation to the functional regions and fiber tracts were determined for both RT plans. Anatomical and neuro-cognitive functions of OARs were compared based on the values of  $D_{\text{max}}$  and  $D_{\text{mean}}$ .

### Statistical analyses

Wilcoxon's test was used to compare the two plans' parameters. The differences were considered statistically significant at  $P$ -value < 0.05 (via SPSS software ver. 25.0).

### Results

The patient characteristics are shown in Table 1.

In this study, the functional regions and fiber tracts that overlap with the target volume were eliminated due to the priority of tumor treatment. The prescribed dose and the dose that covered 95% of the PTV ( $D_{95}$ ) are shown in Table 2. PTV received more than 95% of the prescribed dose for all patients, both for the original and optimized plan (Figure 2).

The maximum and the mean dose to the anatomical OARs are shown in Table 3. The doses received by the anatomical OARs did not exceed the permissible values, both for the optimized and original plans.

**Table 1:** Patient characteristics

| Patient | Gender | Age of diagnosis (y) | Lesion location | Tumor type | Grade |
|---------|--------|----------------------|-----------------|------------|-------|
| 1       | Male   | 29                   | F-T             | Glioma     | High  |
| 2       | Female | 24                   | F               | Glioma     | Low   |
| 3       | Male   | 58                   | T               | Glioma     | Low   |
| 4       | Female | 26                   | P               | Glioma     | Low   |
| 5       | Female | 21                   | F-P             | Glioma     | High  |
| 6       | Female | 54                   | P               | Glioma     | Low   |
| 7       | Female | 63                   | F               | Glioma     | High  |
| 8       | Female | 34                   | F-P             | Glioma     | High  |

F: Frontal, T: Temporal, P: Parietal

The details of the mean and maximum dose reduction to each patient’s functional areas and fiber tracts are presented in Table 4. The dose-volume histogram of the patient with number 8 demonstrates the feasibility of dose reduction in the right optic radiation and left-

hand motor without the PTV dose coverage changing (Figure 3).

The results indicated that the average reduction of the mean and maximum doses to the optimized plans’ functional areas was 25.36% ( $P=0.005$ ) and 18% ( $P=0.005$ ), respectively.

**Table 2:** The prescription dose and D95 of the Planning target volume (PTV)

|           | Prescription Dose (Gy) | D95 of the PTV in the plan without fMRI & DTI (Gy) | D95 of the PTV in plan with fMRI & DTI (Gy) | P-value |
|-----------|------------------------|--|---|---------|
| Patient 1 | 60                     | 57.81  | 57.62                                       | 0.293   |
| Patient 2 | 54                     | 52.15  | 51.87                                       |         |
| Patient 3 | 54                     | 52.18  | 52.41                                       |         |
| Patient 4 | 54                     | 52.38  | 51.36                                       |         |
| Patient 5 | 60                     | 58.09  | 58.37                                       |         |
| Patient 6 | 54                     | 52.36  | 52.72                                       |         |
| Patient 7 | 60                     | 58.64  | 57.51                                       |         |
| Patient 8 | 60                     | 59.45  | 58.18                                       |         |
| SD        | 3.21                   | 3.36   | 3.15  |         |
| Median    | 57                     | 55.10  | 55.12                                       |         |

SD: Standard Deviation, D95: Dose that covered 95% of the PTV, PTV: Planning Target Volume, fMRI: Functional Magnetic Resonance Imaging, DTI: Diffusion Tensor Imaging

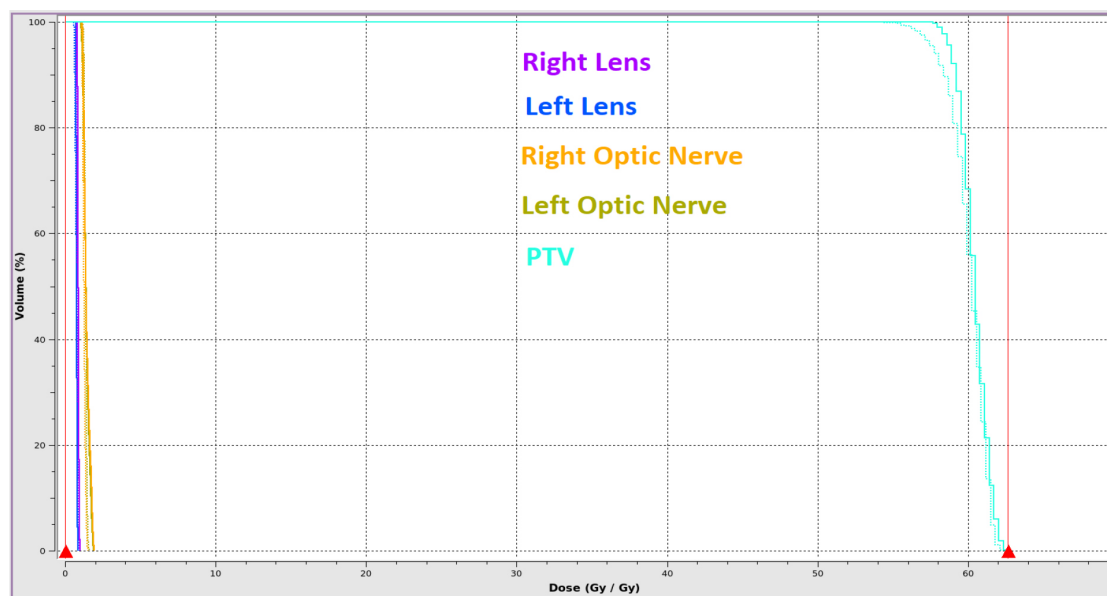


**Figure 2:** Dose-volume histograms (DVH) for patient number 7 showing DVH curves for planning target volume (PTV), optic nerves, and lenses. (The solid line indicates the original plan and the dashed line shows the optimized plan).

**Table 3:** Maximum and mean dose to anatomical organs at risk (OARs)

| Anatomical OARs   | Maximum Dose in the original plan (Gy) | Maximum Dose in optimized plan (Gy) | Mean Dose in the original plan (Gy) | Mean Dose in optimized plan (Gy) |
|-------------------|--|-------------------------------------|-------------------------------------|----------------------------------|
| Brain Stem        | 32.68                                  | 30.80                               | 5.04                                | 3.68                             |
| Optic Chiasm      | 26.17                                  | 22.44                               | 13.74                               | 11.29                            |
| Left Optic Nerve  | 9.84                                   | 12.77                               | 5.43                                | 6.01                             |
| Right Optic Nerve | 4.25                                   | 3.08                                | 2.83                                | 2.59                             |
| Left cochlea      | 2.34                                   | 2.96                                | 1.97                                | 2.44                             |
| Right cochlea     | 1.70                                   | 1.12                                | 1.48                                | 0.99                             |
| Left eye          | 5.34                                   | 8.97                                | 2.30                                | 3.52                             |
| Right eye         | 2.13                                   | 2.60                                | 1.73                                | 2.14                             |

OARs: Organs at risk

In addition, on average, we achieved 15.59% ( $P=0.028$ ) and 20.84% ( $P=0.018$ ), reductions in the mean and maximum doses, respectively, for the optimized plans' fiber tracts. In summary, the results showed a significant dose reduction in the functional structure and fiber tracts while radiotherapy PTV maintained the prescribed dose. Moreover, the anatomical OARs were strictly kept within the acceptable dose tolerance.

## Discussion

While radiation therapy has dramatically improved local control and prolonged progression-free patient survival in some cancer types like primary brain tumor, radiation-induced cognitive impairment is considered a late effect of radiation therapy (RT) in most brain tumor patients because of neuro-cognitive areas' high doses receiving [1-3]. Neurocognitive function damage is one of the cranial irradiation's most crucial side effects that play an essential role in cognitive function and QOL [7,8]. Affected cognitive domains involve IQ scores, learning, memory, processing speed, attention, and executive functioning with a consequent increasing need for rehabilitation interventions [4]. Furthermore, neuropsychological

effects may include social, emotional, and behavioral disorders [5], leading to a significantly decreased QOL than peers [6]. Radiation-induced brain injury, including inflammation, angiogenesis, and cell death, can result in white and grey matter dysfunctions [7] and RT brain damage, causing demyelination (or structural degradation) of axon fibers and disruption of trans-synaptic communications [8]. These injuries may lead to severe irreversible neurological consequences without any visible sign on conventional neuroimaging and histopathology [9], and they harm the QOL and daily functioning [10]. Currently, knowledge about cognitive dysfunction following cranial radiation is limited [12]. However, 19% to 83% of fractionated radiotherapy survivors exhibit disabling and progressive cognitive dysfunction [1]. In this study, we demonstrated the consideration of functional structures and fiber tracts during treatment planning could clinically reduce the radiation doses and neurocognitive complications and increase the patient's life expectancy QOL. Liu et al. reported an innovative method to combine the fMRI brain activation map for stereotactic radiosurgery (SRS) plans. In the SRS plan, direct exposure to the eloquent cor-

**Table 4:**  $D_{\text{mean}}$  and  $D_{\text{max}}$  to the Functional Activation Areas and Fiber Tracts

|                  | $D_{\text{mean}}$ in the original plan (Gy)     | $D_{\text{mean}}$ in the optimized plan (Gy) | $D_{\text{max}}$ in the original plan (Gy) | $D_{\text{max}}$ in the optimized plan (Gy) |       |
|------------------|---|--|--|---|-------|
| Functional areas | Right Hand Motor                                | 23.94  | 18.99                                      | 30.29                                       | 24.76 |
|                  | Left Hand Motor                                 | 30.65  | 21.78                                      | 38.44                                       | 28.94 |
|                  | Right Lip Motor                                 | 31.33  | 24.20                                      | 33.29                                       | 28.29 |
|                  | Left Lip Motor                                  | 25.35  | 16.87                                      | 33.52                                       | 26.58 |
|                  | Right Tongue Motor                              | 23.30  | 18.59                                      | 26.82                                       | 21.71 |
|                  | Left Tongue Motor                               | 20.43  | 13.18                                      | 26.46                                       | 21.91 |
|                  | Right Broca                                     | 55.38  | 50.77                                      | 57.06                                       | 56.52 |
|                  | Left Broca                                      | 11.06  | 5.51                                       | 14.98                                       | 6.54  |
|                  | Right Wernicke                                  | 23.36  | 16.91                                      | 34.18                                       | 28.04 |
|                  | Left Wernicke                                   | 8.67   | 2.38                                       | 7.98  | 3.46  |
|                  | Mean  | 25.35  | 18.92                                      | 30.30                                       | 24.68 |
|                  | SD  | 12.83  | 13.10                                      | 13.23                                       | 14.36 |
|                  | Median  | 23.65  | 17.75                                      | 31.79                                       | 25.67 |
| Fiber tracts     | Right Corticospinal Tract                       | 10.24  | 5.32                                       | 15.07                                       | 8.62  |
|                  | Left Corticospinal Tract                        | 36.14  | 32.89                                      | 55.54                                       | 55.59 |
|                  | Right Frontal Aslant Tract                      | 14.24  | 8.87                                       | 36.57                                       | 27.12 |
|                  | Left Frontal Aslant Tract                       | 27.42  | 24.84                                      | 47.55                                       | 43.90 |
|                  | Right Geniculocalcarine tract (Optic Radiation) | 14.69  | 8.64                                       | 30.81                                       | 25.83 |
|                  | Left Geniculocalcarine tract (Optic Radiation)  | 15.09  | 12.95                                      | 49.74                                       | 46.03 |
|                  | Right Uncinate Fasciculus                       | 13.02  | 10.06                                      | 53.52                                       | 36.70 |
|                  | Mean  | 18.69  | 14.80                                      | 41.26                                       | 34.83 |
|                  | SD  | 9.43   | 10.14                                      | 14.62                                       | 15.65 |
|                  | Median  | 14.69  | 10.06                                      | 47.55                                       | 36.70 |

SD: Standard Deviation

tex through multiple radiation arcs or static radiation IMRT beams was avoided, and the average dose of the eloquent cortex was reduced to 32% [24]. Pantelis et al. demonstrated that with the help of the integration of BOLD-fMRI and DTI into CyberKnife SRS can be considered and spared critical brain structures [16]. Wang et al. integrated BOLD-fMRI and DTI data in radiation treatment plans of 20 patients with high-grade glioma. fMRI and DTI data were derived from the primary motor cortex and the corticospinal tract, respectively [4]. Wang et al. have found that the  $D_{\text{max}}$  and  $D_{\text{mean}}$

of the ipsilateral and contralateral PMC and CST regions considerably decreased [4]. The fMRI and DTI data of 16 patients with brain tumors applied in CyberKnife radiosurgery by Sun et al. fMRI data were obtained from the speech area and DTI data from the pyramidal tracts. It was observed that the maximum dose was reduced by 22.71% on average in the functional area [20].

Rhodes et al. used resting-state fMRI data from 9 patients with primary brain tumors in their radiation therapy plans. Functional data in the default mode network (DMN) was

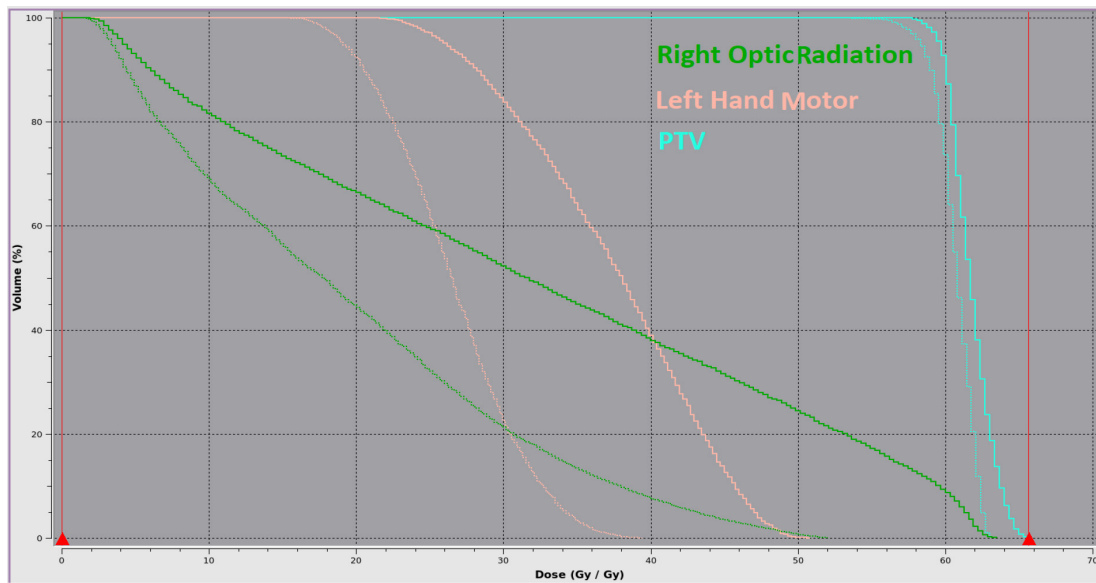


**Figure 3:** Dose-volume histograms (DVH) for patients with number 8 showing DVH curves to the planning target volume (PTV), right optic radiation, and left-hand motor cortex. (The solid line indicates the original plan and the dashed line shows the optimized plan)

obtained from resting-state fMRI. Moreover, they achieved 20% ( $P=0.002$ ) and 12% ( $P=0.002$ ) reductions in the mean and maximum doses, respectively, to the DMN [25].

Several functional areas and neural tracts were found in the present study based on the tumor site and functional performance. The required dose was significantly reduced in the optimized plan by considering the tumor site based on the functional areas and neural tracts.

In most similar studies, the radiation therapy design considered the same functional area and a neural tract for all patients [24]. Our study treatment plans found several functional areas and neural tracts according to each patient's tumor site and functional performance. The integration of fMRI and diffusion tensor imaging in radiation treatment planning has many challenges and limitations, which were more complex for patients with brain tumors.

Functional tasks for imaging data acquisition add functional OARs and neural tracts which is challenging for the participants, besides the high-cost advanced imaging, and

time-consuming and complicated treatment plans. Large tumor volume may limit the radiation treatment plan, which is challenging to fully encompass PTV by 95% of the prescribed dose while minimizing the dose delivered to the specified OARs. As a result, high-risk functional areas and neural tracts may not be considered in radiation treatment plans.

Neurocognitive complications are long-term side effects of radiation with the lowest risk for short-term survival; patient survival should also be considered. In the case of short-term survival, involving the patient with advanced image acquisition, which adds additional cost and complexity, is useless. Therefore, patients with proper general health conditions, local tumors, and relatively long survival are the best cases for advanced treatment planning using fMRI and DTI. The future of cancer radiotherapy will depend on the usage of advanced imaging in modern treatment planning techniques. The improvement of combination precision will be associated with more beneficial and effective treatment. Results of the

present study can provide the basis for future clinical follow-up studies to more accurately investigate the impacts of dose reduction on neurological-cognitive complications. This study has some limitations, including the small sample size due to the limited number of accessible patients, the lack of cooperation of the patients during fMRI and DTI lengthy imaging procedures, and the expansive tumor growth which made it impossible to implement an optimized treatment design.

## Conclusion

The functional regions and fiber tracts should be considered in the radiation treatment planning for patients with brain tumors, leading to decreasing a notable dose to the critical areas to preserve the unique function of the brain without compromising the PTV coverage or sparing anatomical OARs. For the clinical use of the functional regions and fiber tracts in radiation treatment planning, there is no need to combine the functional regions and fiber tracts in radiation treatment planning for all patients with brain tumors. Several factors, such as tumor type, grade, and location together with the patient's age, survival, and physical status should be considered. However, a proprietary integration of fMRI and DTI into radiation treatment planning is possible, necessary, and valuable, a team of neurologists, radiologists, medical physicists, and radiation oncologists should determine its necessity.

## Authors' Contribution

All authors contributed to the study's conception, methodology, and design. Material preparation and data collection were performed by A. Boroun and H. Gholamhosseinian. Data analysis was performed by A. Boroun and A. Montazerabadi. The main manuscript text was written by A. Boroun and F. Pashaei. A. Montazerabadi (medical physicist-MRI) and SH. Molana (Radiation oncologist) and H. Gholamhosseinian (medical physicist-radiation therapy) reviewed and edited the pa-

per according to their field. All authors read, modified, and approved the final version of the manuscript.

## Ethical Approval

The AJA University of Medical Sciences Ethics Committee approved the study's protocol (Ethic code: IR.AJAUMS.REC.1399.255).

A preprint of the study was posted at <https://www.researchsquare.com/article/rs-1373965>.

## Informed consent

All the participants have written informed consent in the project.

## Conflict of Interest

None

## References

1. Sontheimer H. Brain Tumors. In: Diseases of the Nervous System. San Diego: Academic Press; 2015. p. 259-88.
2. Pignatti F, Van Den Bent M, Curran D, Debruyne C, Sylvester R, Therasse P, et al. Prognostic factors for survival in adult patients with cerebral low-grade glioma. *J Clin Oncol*. 2002;**20**(8):2076-84. doi: 10.1200/JCO.2002.08.121. PubMed PMID: 11956268.
3. Chang J, Narayana A. Functional MRI for radiotherapy of gliomas. *Technol Cancer Res Treat*. 2010;**9**(4):347-58. doi: 10.1177/153303461000900405. PubMed PMID: 20626201.
4. Wang M, Ma H, Wang X, Guo Y, Xia X, Xia H, et al. Integration of BOLD-fMRI and DTI into radiation treatment planning for high-grade gliomas located near the primary motor cortexes and corticospinal tracts. *Radiat Oncol*. 2015;**10**:64. doi: 10.1186/s13014-015-0364-1. PubMed PMID: 25884395. PubMed PMCID: PMC4357178.
5. Makale MT, McDonald CR, Hattangadi-Gluth JA, Kesari S. Mechanisms of radiotherapy-associated cognitive disability in patients with brain tumours. *Nat Rev Neurol*. 2017;**13**(1):52-64. doi: 10.1038/nrneurol.2016.185. PubMed PMID: 27982041. PubMed PMCID: PMC5805381.
6. Baron Nelson M, Compton P, Patel SK, Jacob E, Harper R. Central nervous system injury and neurobiobehavioral function in children with

- brain tumors: a review of the literature. *Cancer Nurs.* 2013;**36**(2):E31-47. doi: 10.1097/NCC.0b013e31825d1eb0. PubMed PMID: 22781957. PubMed PMCID: PMC5964978.
7. Son Y, Yang M, Wang H, Moon C. Hippocampal dysfunctions caused by cranial irradiation: a review of the experimental evidence. *Brain Behav Immun.* 2015;**45**:287-96. doi: 10.1016/j.bbi.2015.01.007. PubMed PMID: 25596174.
  8. Liu R, Page M, Solheim K, Fox S, Chang SM. Quality of life in adults with brain tumors: current knowledge and future directions. *Neuro Oncol.* 2009;**11**(3):330-9. doi: 10.1215/15228517-2008-093. PubMed PMID: 19001097. PubMed PMCID: PMC2718978.
  9. McDuff SG, Taich ZJ, Lawson JD, Sanghvi P, Wong ET, Barker FG, et al. Neurocognitive assessment following whole brain radiation therapy and radiosurgery for patients with cerebral metastases. *J Neurol Neurosurg Psychiatry.* 2013;**84**(12):1384-91. doi: 10.1136/jnnp-2013-305166. PubMed PMID: 23715918.
  10. Bailey CC, Gnekow A, Wellek S, Jones M, Round C, Brown J, et al. Prospective randomised trial of chemotherapy given before radiotherapy in childhood medulloblastoma. International Society of Paediatric Oncology (SIOP) and the (German) Society of Paediatric Oncology (GPO): SIOP II. *Med Pediatr Oncol.* 1995;**25**(3):166-78. doi: 10.1002/mpo.2950250303. PubMed PMID: 7623725.
  11. Gkogkou P, Ajithkumar TV. Advances in Radiotherapy for Pediatric Brain Tumours. In: *Pediatric Neurosurgery for Clinicians*. Cham: Springer International Publishing; 2022. p. 813-38.
  12. Padovani L, André N, Constine LS, Muracciole X. Neurocognitive function after radiotherapy for paediatric brain tumours. *Nat Rev Neurol.* 2012;**8**(10):578-88. doi: 10.1038/nrneurol.2012.182. PubMed PMID: 22964509.
  13. Macedoni-Luksic M, Jereb B, Todorovski L. Long-term sequelae in children treated for brain tumors: impairments, disability, and handicap. *Pediatr Hematol Oncol.* 2003;**20**(2):89-101. doi: 10.1080/0880010390158595. PubMed PMID: 12554520.
  14. Ajithkumar T, Price S, Horan G, Burke A, Jefferies S. Prevention of radiotherapy-induced neurocognitive dysfunction in survivors of paediatric brain tumours: the potential role of modern imaging and radiotherapy techniques. *Lancet Oncol.* 2017;**18**(2):e91-100. doi: 10.1016/S1470-2045(17)30030-X. PubMed PMID: 28214420.
  15. Rutkowski S, Bode U, Deinlein F, Ottensmeier H, Warmuth-Metz M, Soerensen N, et al. Treatment of early childhood medulloblastoma by postoperative chemotherapy alone. *N Engl J Med.* 2005;**352**(10):978-86. doi: 10.1056/NEJ-Moa042176. PubMed PMID: 15758008.
  16. Pantelis E, Papadakis N, Verigos K, Stathochristopoulou I, Antypas C, Lekas L, et al. Integration of functional MRI and white matter tractography in stereotactic radiosurgery clinical practice. *Int J Radiat Oncol Biol Phys.* 2010;**78**(1):257-67. doi: 10.1016/j.ijrobp.2009.10.064. PubMed PMID: 20421146.
  17. Stancanello J, Cavedon C, Francescon P, Causin F, Avanzo M, Colombo F, et al. BOLD fMRI integration into radiosurgery treatment planning of cerebral vascular malformations. *Med Phys.* 2007;**34**(4):1176-84. doi: 10.1118/1.2710326. PubMed PMID: 17500448.
  18. Maruyama K, Kamada K, Shin M, Itoh D, Masutani Y, Ino K, et al. Optic radiation tractography integrated into simulated treatment planning for Gamma Knife surgery. *J Neurosurg.* 2007;**107**(4):721-6. doi: 10.3171/JNS-07/10/0721. PubMed PMID: 17937214.
  19. Maruyama K, Kamada K, Ota T, Koga T, Itoh D, Ino K, et al. Tolerance of pyramidal tract to gamma knife radiosurgery based on diffusion-tensor tractography. *Int J Radiat Oncol Biol Phys.* 2008;**70**(5):1330-5. doi: 10.1016/j.ijrobp.2007.08.010. PubMed PMID: 17935904.
  20. Sun L, Qu B, Wang J, Ju Z, Zhang Z, Cui Z, et al. Integration of Functional MRI and White Matter Tractography in CyberKnife Radiosurgery. *Technol Cancer Res Treat.* 2017;**16**(6):850-6. doi: 10.1177/1533034617705283. PubMed PMID: 28425348; PMCID: PMC5762040.
  21. Fiscaro R, Nicole M. Functional MRI: Petrovich Brennan and Andrei I Holodny. Chapter 29. In *Handbook of Neuro-Oncology Neuroimaging*. 2nd Edition. San Diego: Academic Press; 2016. p. 317-325.
  22. Shevzov-Zebrun N, Brennan NM, Peck KK, Holodny AI. Advanced Functional Imaging: fMRI, PET, and MEG. In: *Image-Guided Neurosurgery*. Academic Press; 2015. p. 63-89.
  23. Mahdavi A, Houshmand S, Oghabian MA, Zarei M, Mahdavi A, Shoar MH, Ghanaati H. Developing optimized fMRI protocol for clinical use:

- comparison of different language paradigms. *J Magn Reson Imaging*. 2011;**34**(2):413-9. doi: 10.1002/jmri.22604. PubMed PMID: 21780233.
24. Liu WC, Schulder M, Narra V, Kalnin AJ, Cathcart C, Jacobs A, et al. Functional magnetic resonance imaging aided radiation treatment planning. *Med Phys*. 2000;**27**(7):1563-72. doi: 10.1118/1.599022. PubMed PMID: 10947259.
25. Sours Rhodes C, Zhang H, Patel K, Mistry N, Kwok Y, D'Souza WD, et al. The Feasibility of Integrating Resting-State fMRI Networks into Radiotherapy Treatment Planning. *J Med Imaging Radiat Sci*. 2019;**50**(1):119-28. doi: 10.1016/j.jmir.2018.09.003. PubMed PMID: 30777232.